

Molecular dynamics simulation of argon using a 6-12 Lennard-Jones potential

HANS LANGERAK[†] AND SEBASTIAAN HERMANS[‡]

[†]4592344, MSc Applied Physics, Delft University of Technology, Lorentzweg 1, 2628 CJ, The Netherlands

[‡]4582608, MSc Applied Physics, Delft University of Technology, Lorentzweg 1, 2628 CJ, The Netherlands

April 1, 2020

In this paper, we present a molecular dynamics simulation of a system of up to 500 argon atoms, interacting through a 6-12 Lennard-Jones potential. The equations of motion are solved numerically using the velocity-Verlet algorithm as a symplectic integrator, ensuring energy conservation within our closed system. The minimal image convention is used to emulate an infinite system. After a period of equilibration, the simulation reached a state of thermal equilibrium at the initially set temperature in which energy was conserved. The simulated pair correlation function agreed very well with the theoretical expectation for the solid, liquid and gaseous phase. Results for the compressibility and the heat capacity were largely consistent with literature values. This simulation shows, once again, that a system interacting through a two-body potential can be very useful in studying the properties of argon.

1. INTRODUCTION

Interacting systems are the most common systems around us, yet they are impossible to study analytically due to their complexity. Therefore, numerical methods are used to study these systems. This can give insight into many thermodynamic properties, such as when phase transitions occur.

In this paper, a molecular dynamics simulation is presented of a system of argon atoms, interacting through a 6-12 Lennard-Jones potential. Different physical quantities are explored to check the validity of the simulation, including the pair correlation for different phases of argon, compressibility and the specific heat. Previous research into the study of argon systems has been performed by Lebowitz et al. [1] and L. Verlet [2], in which the same thermodynamic quantities were studied. We investigate the behaviour of argon systematically and quantitatively, and try to validate our results with the help of this previous research.

2. METHOD

A. The physical model

Within the simulation, the argon atoms interact through the Lennard-Jones (LJ) potential. The LJ potential provides a mathematical model for the interaction between neutral particles as a function of the distance between them. It has been found to provide a proper approximation for interaction between neutral atoms, especially for argon [2]. The expression for the LJ potential is given as [3]

$$U(r) = 4 \cdot \epsilon \left[\left(\frac{\sigma}{r} \right)^{12} - \left(\frac{\sigma}{r} \right)^6 \right], \quad (1)$$

and a depiction of the LJ potential can be found in figure 1. The LJ potential consists of two terms, the first being the exchange interaction between two particles. This term describes a repulsive force as a result of the Pauli exclusion principle for two identical fermionic particles. It scales with r^{-12} , where r is the interatomic distance. The second term describes an attractive force between particles as a result of Van der Waals forces and scales with r^{-6} . Consequently, the repulsive force for relatively small interatomic distances is very large compared to the attractive force. At larger distances however the attractive force becomes the predominant term. Because of the powers to the sixth and to the twelfth, this expression of the LJ potential is also called the 6-12 LJ potential. ϵ gives the minimum value of the potential well, which is reached somewhere in between these two extremes. σ in the LJ potential gives the distance at which the potential is zero.

The resulting force on each particle labeled i can be expressed with Newton's second law,

$$m \frac{d^2 \underline{x}_i}{dt^2} = \underline{F}(\underline{x}_i) = -\nabla U(\underline{x}_i), \quad (2)$$

where the potential U is given by the LJ potential.

B. Natural units

To prevent round-off errors in the simulation, to make the calculations less cumbersome and to provide better insight into expected unit scales in the simulation, the simulation uses natural units instead of the normal SI units. These natural units are chosen in such a way that they represent characteristic scales

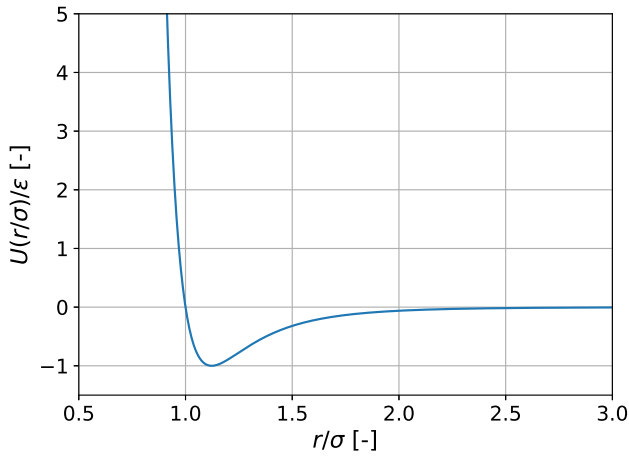


Fig. 1. Lennard-Jones potential as a function of the interatomic distance divided by σ , σ being the distance at which the potential is zero. The repulsive force dominates for small interatomic distances r , whereas for larger distances the attractive force dominates. The minimum value of the resulting potential well, $-\epsilon$, can be found at approximately 1.122σ .

for argon. From the LJ potential we use σ to define $\tilde{x} = x/\sigma$ as our dimensionless unit for distance. ϵ from the LJ potential is chosen as characteristic energy in the system. This way the dimensionless LJ potential becomes

$$\tilde{U}(\tilde{r}) = U(r)/\epsilon = 4 \cdot (\tilde{r}^{-12} - \tilde{r}^{-6}). \quad (3)$$

Using the mass of an argon atom at the unit mass, $\tilde{m} = m/m_{\text{argon atom}}$, rewriting Newton's second law for some particle labeled i then becomes

$$\frac{d^2 \tilde{x}_i}{d\tilde{t}^2} = \frac{1}{\sigma} \frac{d^2 x_i}{dt^2} = \frac{-1}{m\sigma} \nabla U(r_i) = \frac{-\epsilon}{m\sigma} \nabla \tilde{U}(\tilde{r}_i) = \frac{-\epsilon}{m\sigma} \tilde{\nabla} \tilde{U}(\tilde{r}_i). \quad (4)$$

We can use equation 4 to define a dimensionless time, namely $\tilde{t} = t / \left(\frac{m\sigma^2}{\epsilon} \right)^{1/2}$. The velocity can now be expressed in dimensionless units as

$$\tilde{v} = v / \sqrt{\epsilon/m} = \sqrt{3k_B T / \epsilon}. \quad (5)$$

With this last expression the kinetic energy can also be expressed using only the dimensionless velocity, as

$$\tilde{E}_{\text{kin}} = \frac{1}{2} \tilde{v}^2. \quad (6)$$

Lastly, using the characteristic energy ϵ , we can also define a dimensionless temperature,

$$\tilde{T} = T / (\epsilon/k_B). \quad (7)$$

For the rest of this paper, the tildes indicating dimensionless parameters will be omitted, i.e. the dimensionless temperature will be written as T .

C. Minimal image convention

As we are interested in the behavior of argon in different phases, most preferably we would want to simulate an infinite system of argon atoms, simulating real life argon systems as best as possible. Computationally, however, this is not doable. In

order to emulate an infinite system of argon atoms, a system is simulated within a box with length L into each dimension, and with periodic boundary conditions. This box then would behave as if it was surrounded by an infinite system of the same exact boxes, all with the same physics going on inside. For this it is required that a constant volume of the box is set, with a constant number of particles inside.

For a particle moving in the box, the periodic boundary conditions mean that when the particle arrives at the boundary of the box, it re-enters at the opposite side of the box it is currently in. For the force acting on the particles in the system, this also has consequences. Instead of calculating the force on every particle due to every other particle in the infinite system, in the simulation only the forces due to a particle's nearest 'image partners' are considered. This means that for the force calculation on a particular particle, only particles are considered that are the most nearby copies of those same particles either within the simulation box or in one of the surrounding boxes, depending on in whichever box the particles are closest to the particle considered. A depiction of this so called 'minimal image convention' can be found in figure 2.

The choice for the minimal image convention can be justified by looking at the LJ potential in equation 1: the force falls off quickly as a function of the distance between two particles.

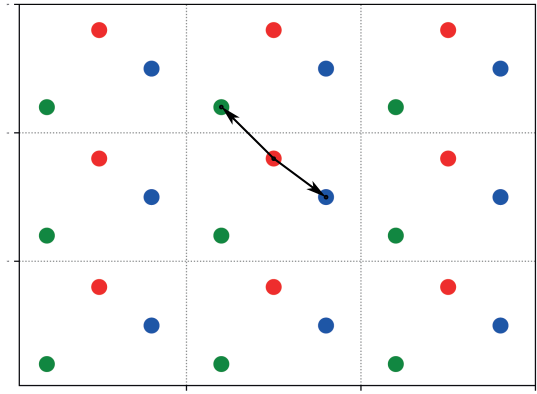


Fig. 2. Depiction of the minimal image convention. Within the middle box, the red particle experiences a force only from the blue particle in the same box and the green particle in the box above. The green particle in the middle box does not contribute to the force on the red particle.

D. Initialization

To simulate a system of interacting argon atoms, the atoms are initialised in an fcc lattice, as depicted in figure 3. This is the crystal structure that argon forms in its solid state, and enables us to simulate phase transitions. It also prevents the atoms from being initialised too closely together, which would bring about a relatively large increase in energy of the atoms as a result of the repulsive LJ potential. The number of particles N in the system is chosen according to the size of the system, so it is compatible with an fcc lattice.

For the fcc lattice the periodic boundary conditions mean that it is initialised in such a way that it would be completed if the box where to be simulated in the described infinite system. Additionally, the particles are not initialised exactly on the boundaries of the box, but with an offset of a quarter of the lattice parameter. This was done to avoid potential rounding errors in the simulation as a result of counting particles that actually belong in a neighbouring box.

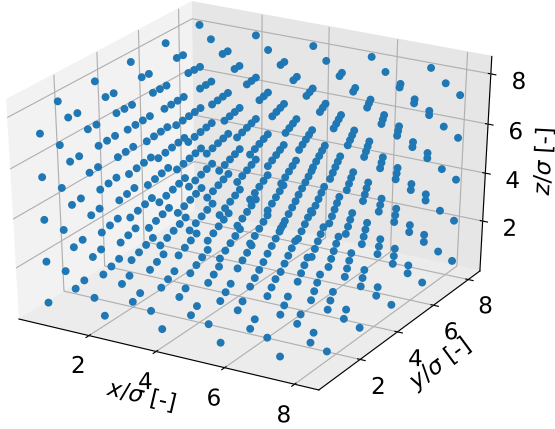


Fig. 3. FCC lattice as initialised in a simulation of 500 particles. It consists of five copies of the primitive unit cell into each dimension. Due to the periodic boundary conditions, the fcc lattice is not totally completed at the boundaries.

The initial velocities of the particles in the system are chosen using a Gaussian distribution (using dimensionless parameters),

$$P(v_{x,y,z}) = \sqrt{\frac{m}{2\pi T}} e^{-\frac{mv_{x,y,z}^2}{2T}}, \quad (8)$$

in order to generate a Maxwell-Boltzmann distribution. As the system should have no net momentum, the velocities are rescaled after initialisation by subtracting the mean velocity from all velocities. This way, the resulting mean velocity of the system equals zero.

E. Verlet algorithm

Newton's second law as given by equation 4 cannot be solved analytically for the given system. Therefore, a numerical integration scheme is required to determine the time evolution of the trajectory of the particles. As our mechanical system has a constant volume and a constant amount of particles, and undergoes no exchange with its environment, it should contain a constant total amount of energy, and should thus be able to be described within the micro-canonical ensemble. Under time evolution by numerical integration of the equations of motion, the energy should thus also be preserved. For this an integrator is used that has the special property called symplecticity, which ensures conservation of (a discrete version of) the total energy [4]. For our purpose, the symplectic integrator used is the velocity-Verlet algorithm [2]. By performing Taylor expansions of $\underline{x}(t+h)$, $\dot{\underline{x}}(t+h)$ and $\ddot{\underline{x}}(t+h)$, the velocity-Verlet algorithm can be found to be

$$\underline{x}(t+h) = \underline{x}(t) + h\dot{\underline{x}}(t) + \frac{h^2}{2}\ddot{\underline{x}}(t) \quad (9)$$

for a particle's position at one time step later and

$$\dot{\underline{x}}(t+h) = \dot{\underline{x}}(t) + \frac{h}{2}(F(\underline{x}(t+h)) + F(\underline{x}(t))) \quad (10)$$

for a particle's velocity at one time step later.

F. Rescaling

The simulation uses a desired density and temperature as initial input. After the simulation has been started the system will start equilibrating. Simultaneously however, exchange will occur between the kinetic and potential energies in the system. This will automatically lead to a change in the set temperature via the equipartition theorem, which holds in our system described within the micro-canonical ensemble, from which we know that

$$E_{kin} = (N-1)\frac{3}{2}k_B T. \quad (11)$$

In this simulation, to force the system to the initially set temperature, manual rescaling of the kinetic energy is performed using the parameter λ , given as

$$\lambda = \sqrt{\frac{(N-1)3k_B T}{\sum_i m v_i^2}}. \quad (12)$$

By comparing the kinetic energy as given by the equipartition theorem, and the kinetic energy currently in the system, λ can be used to get the system to match the set temperature. The square root follows from the square of the velocity in the kinetic energy. λ is used to rescale the velocities of all particles in the system at regular intervals until some set equilibration time, as

$$\underline{v}_i \rightarrow \lambda \underline{v}_i. \quad (13)$$

The total amount of timesteps, the length of one timestep, the equilibration time and the rescaling intervals have been chosen following the approach described in the book by J. Thijsen [5].

G. Physical quantities

We have previously defined that our system can be described within the micro-canonical ensemble. Now we can use our knowledge of the micro-canonical ensemble to find values for different physical quantities. Most importantly, the total energy in the system should be conserved after equilibration. Next to the total energy, we have previously used eq. 11 from the equipartition theory to force the system to thermal equilibrium. After equilibration, the same equation can be used to calculate the temperature of the system, checking whether the system actually is in thermal equilibrium at the set temperature. Also, using the LJ potential, the average potential energy per particle can be determined. As the potential energy per particle is dependent on the thermodynamic and mechanical state the system is in, this value can be used to check the validity of the simulation.

To further our understanding of the simulation and check its validity, there are multiple other thermodynamic quantities that can be determined. Firstly, the pair correlation function, given as [5]

$$g(r) = \frac{2V}{N(N-1)} \frac{\langle n(r) \rangle}{4\pi r^2 \Delta r}, \quad (14)$$

describes the probability of finding a particle at a certain distance from a reference particle, relative to an ideal gas. Here

Δr is the bin size and $n(r)$ a histogram of the particle pair distances. A histogram is generated at every timestep, counting how many particles can be found within a distance $[r, r + \Delta r]$ from each other, using Δr as bin size. The time-averaged histogram is made by time-averaging the sum of all individual histograms.

Based on the form that the pair correlation takes, one can determine the thermodynamic state of the system. For a solid it should give non-zero relative probabilities only at specific distances. This is because the particles are then organized in a lattice configuration, while for a gas it should be almost uniformly distributed because the particles are moving freely. A liquid will give a pair correlation that is a mixture of solid and gaseous pair correlations.

Secondly, the compressibility of a system of N particles is given as [6]

$$\frac{\beta P}{\rho} = 1 - \frac{\beta}{3N} \left\langle \frac{1}{2} \sum_{i,j} r_{ij} \frac{\partial U}{\partial r_{ij}} \right\rangle. \quad (15)$$

The compressibility is a measure of the relative volume change due to a difference in pressure. In eq.15 the part in between the angle brackets is the virial function. The virial function provides a way of calculating the average total kinetic energy for complicated systems that do not have an exact solution, like the one studied here. Furthermore, it is valid even when the system is not in equilibrium. Note that the virial is an ensemble average but in this research it is a time average. This method is valid due to the fundamental postulate of statistical mechanics. The compressibility is a measure of the relative volume change due to a pressure difference.

Finally, the heat capacity of a system described within the micro-canonical ensemble is given as [1]

$$\frac{\langle \delta K^2 \rangle}{\langle K \rangle^2} = \frac{2}{3N} \left(1 - \frac{3N}{2C_V} \right). \quad (16)$$

Here $\langle \delta K^2 \rangle = \langle K^2 \rangle - \langle K \rangle^2$ and K the kinetic energy. Note that these again are time averages instead of ensemble averages. Dividing by the number of particles yields the specific heat of a particle in the system, now given as

$$C_{\text{particle}} = \frac{C_V}{N}. \quad (17)$$

A first check in verifying the correctness of the specific heat of a particle is to determine if the high temperature limit value is in agreement with literature [7]. Furthermore, if we subtract the kinetic part of the specific heat per particle, $\frac{3}{2}$, from eq.17 we get the interaction part of the specific heat per particle $C_{i_{\text{theory}}}$. This quantity has been studied by Lebowitz et al [1] and therefore allows us to further check the validity of our results.

The errors in all determined physical quantities are computed using auto-correlation and standard error propagation methods, with exceptions made for the error in the virial and kinetic energy as these are time averages. To get errors in these quantities we make use of data blocking. In data blocking a set of values is replaced with an averaged version of them, in our case a time averaged value. The amount of values replaced is called the block size. Doing this for all the data then gives multiple blocks

which are subsequently used to calculate the error. This is done using eq. 18, where A is the data blocked quantity.

$$\sigma_A = \sqrt{\langle A^2 \rangle + \langle A \rangle^2} \quad (18)$$

These blocks can, however, still be correlated. To get rid of the correlation the block size is chosen such that the data is no longer correlated. Typically this means that the computed error becomes almost stable after a certain block size is used.

3. RESULTS & DISCUSSION

To check the validity of the simulation, results obtained for the physical quantities described in the method are compared to literature and basic laws of physics, like energy conservation.

If not mentioned explicitly, the number of particles used for the simulations was 500. Of a total of 5000 timesteps of length 0.004, the first 2500 timesteps are used for equilibration with rescaling every 10 timesteps. After equilibration we assume the system to be in a state of equilibrium. We can then use the last 2500 timesteps to find values for different physical quantities.

A. Energy & temperature

A first check of the simulation is whether the total energy is conserved within the system. This is done by checking if the sum of the kinetic and potential energy is relatively constant. A graph of all energies is presented in figure 4. We see that after equilibration the total energy has a constant value of -2003.373 ± 0.008 . Based on this we conclude that the total energy is conserved up to negligible fluctuations.

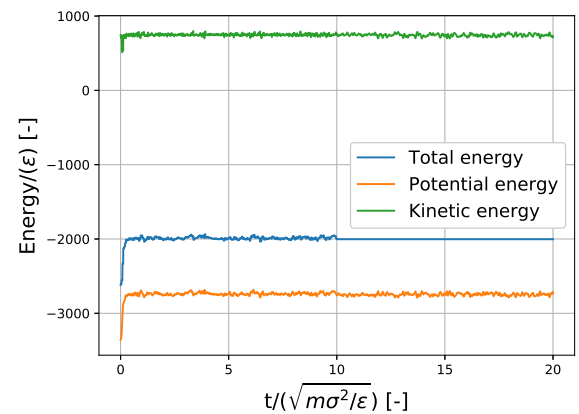


Fig. 4. Total, potential and kinetic energy of a system with 500 particles and an initial temperature T of 1 and density ρ of 0.8. The kinetic energy is rescaled up until timestep 2500, which is seen by the transition to a relatively constant total energy of -2003.373 ± 0.008 at $t=10$.

To see if the system indeed is in thermal equilibrium after equilibration, the average temperature of the system has been calculated for different densities. In addition, the potential energy per particle in those systems was determined. Simulations results, for both 108 and 500 particles, can be found in table 1, where they are compared to values found in the book by J. Thijssen [5]. As it turned out, both systems reached thermal equilibrium after equilibration, but only the system consisting of 108 particles correctly estimated the values of the potential

energy per particle. It seems logical that the potential energy per particle is lower in a system consisting of more particles, as a result of the LJ potential. The difference in the results can probably be explained by a difference in the amount of simulated particles in our simulation and in that of the literature reference.

Table 1. Comparison of the equilibrium temperature and potential energy per particle between literature [5] and the simulation. Results were obtained for varying density ρ , for both 108 and 500 particles, with an initially set temperature $T_0(\epsilon/k_B)$ of 1.0. Both systems seem to be in equilibrium at the set temperature. The simulation of 108 particles estimates the value for the potential energy per particle correctly. The simulation of 500 particles however underestimates the potential energy per particle for all densities.

	$\rho(1/\sigma^3)$	$T(\epsilon/k_B)$	$U(\epsilon)$
Theory	0.88	0.990	-5.704
	0.80	1.010	-5.271
	0.70	1.014	-4.662
N = 108	0.88	0.99 ± 0.02	-5.70 ± 0.03
	0.80	1.02 ± 0.02	-5.27 ± 0.03
	0.70	1.01 ± 0.02	-4.69 ± 0.03
N = 500	0.88	1.000 ± 0.011	-5.90 ± 0.02
	0.80	1.002 ± 0.008	-5.48 ± 0.01
	0.70	1.011 ± 0.008	-4.85 ± 0.01

Results differed per simulation, probably as a result of the fluctuations in the kinetic energy. Due to the fluctuations in the kinetic energy λ kept correcting the velocities in the system, thus never reaching a constant value. Consequently, when the rescaling is stopped at the equilibration time, it differs per simulation at what exact level the kinetic energy is at that moment in time. Prolonging the equilibration period would not have produced better results, as on average the simulation reached a relative equilibrium position far before the equilibration time. Also forcing the lambda factor to converge to 1 would not have produced better results, as the fluctuations are inherent to the system, and forcing it to 1 would not necessarily produce a more valid result. In conclusion, the only way to produce better results would be to reduce the size of the fluctuations.

Fluctuations did get smaller with the number of particles in the simulated system. For 108 particles it is perceived that results differ relatively more than for a simulation using 500 particles. In order to get more consistent results with lower uncertainties the simulated system should thus be scaled up.

B. Pair correlation

The pair correlation has been calculated for three different phases of the argon system: solid, liquid and gas. Figures of the different phases are presented in figures 5, 6 and 7 respectively.

One thing that is shared by all three phases is that the pair correlation has its first peak at 1.09σ for 500 particles. This is close to the expected value of 1.122σ , as that is where the LJ potential has its minimum. The disagreement is probably a result of the number of particles used in the simulation. For 108 and 256 particles the first peaks were at 1.05σ and 1.07σ respectively, approaching the expected value better with the amount of particles simulated.

Figure 5 shows that there are multiple clear peaks, which is what is expected for a solid. This is expected because the atoms are still in the fcc lattice shape, so only specific distances are possible. The peak width of the peaks is due to the vibrations of the particles at the lattice points. Also, an offset is emerging from a distance of 2.5 and onwards, which is also seen in literature [8]. We suspect that this is because, at a larger distance, more particles are vibrating in and out of their respective bins, relative to the reference particle. Due to this they enter a neighbouring bin resulting in some overlap between bins and thus the offset. Possible reasons why this is not visible at shorter distances is because the amount of particles is still too small for any visible effect and the particles could still be separated too much from each other for any effect.

Next, figure 6 shows a large peak and then two smaller ones, after which the pair correlation flattens out to an average value of 1, as is expected for a liquid based on [5].

Finally, figure 7 again shows a large peak at 1.09σ due to the minimum of the Lennard-Jones potential. However, beyond this distance the particles behave as free particles because the strength of the Lennard-Jones potential is negligible. Thus, the pair correlation function goes to 1 as this is now essentially an ideal gas with respect to the particle considered.

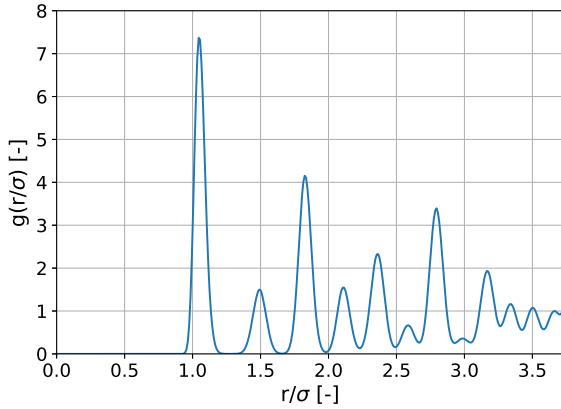


Fig. 5. Pair correlation function for a solid with temperature $T = 0.5$ and density $\rho = 1.2$, simulated with a system of 500 particles. The first peak is at 1.09σ due to the Lennard-Jones potential minimum. From 2.5σ and onwards the pair correlation no longer goes to zero but has an offset. This is due to the particles vibrating in and out of their respective bins. Increasing the distance further results in counting more particles, increasing the probability of particles vibrating in and out of neighboring bins, further increasing the offset up to 3.5σ .

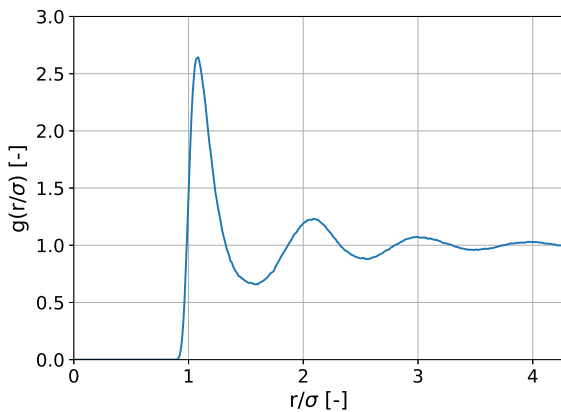


Fig. 6. Pair correlation function for a liquid with temperature $T = 1$ and density $\rho = 0.8$, simulated with a system of 500 particles. The first peak appears at 1.09σ due to the Lennard-Jones potential minimum after which the pair correlation slowly moves to that of an ideal gas at 3σ . This is because the interaction due to the potential between the pairs is negligible at this distance.

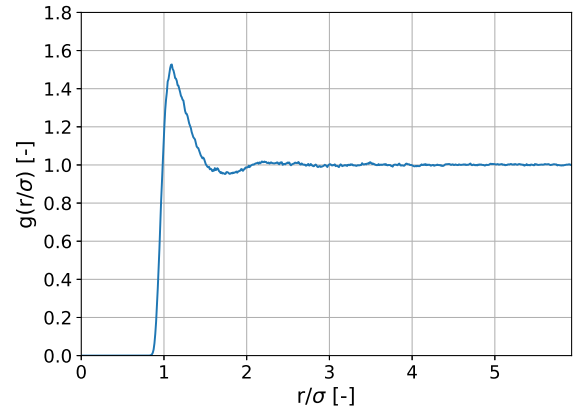


Fig. 7. Pair correlation function for a gas with $T=3$ and density $\rho = 0.3$, simulated with a system of 500 particles. At 1.09σ a large peak is present, due to the Lennard-Jones potential minimum. Shortly after this the particles start behaving like an ideal gas as the pair correlation moves to 1.

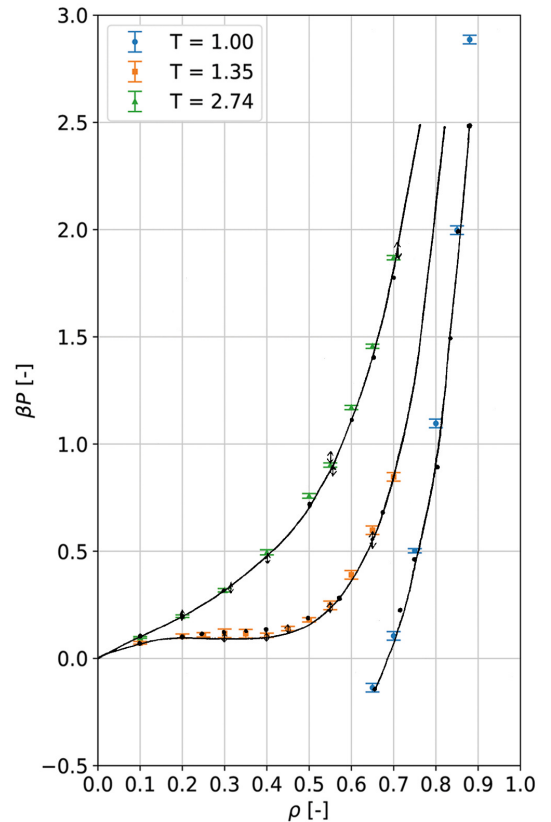


Fig. 8. βP as a function of ρ , for isotherms $T = 2.74$, $T = 1.35$ and $T = 1.00$. Results are compared with simulation results with a LJ potential by L. Verlet (solid lines) [2], Monte Carlo simulations with a LJ potential (arrows) [9], and experimental results in argon (dots) [10][11][12]. Our results show great correspondence with literature values for the isotherms $T = 2.74$ and $T = 1.35$. For $T = 1.00$ βP is overestimated as a function of ρ .

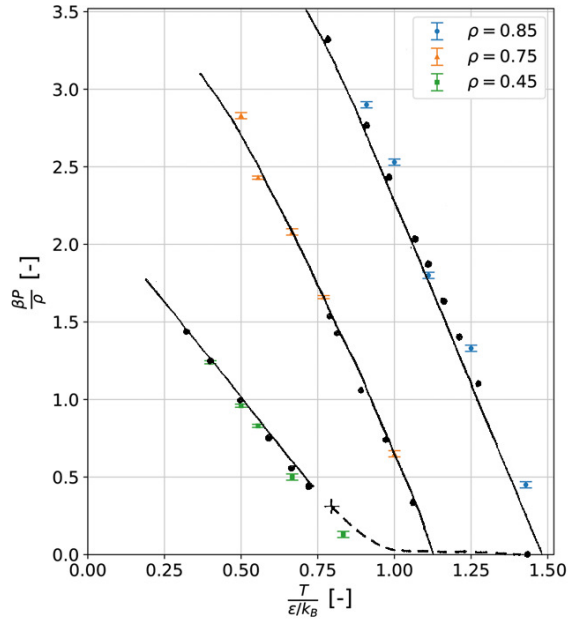


Fig. 9. Compressibility as a function of temperature for $\rho = 0.85$, $\rho = 0.75$ and $\rho = 0.45$. The results are compared with simulations by L. Verlet (solid lines) [2] and experimental values in argon [10][11][12]. The dashed curve corresponds to the gas-liquid and solid-fluid coexistence line. The shape of the simulation results corresponds well to the simulation by L. Verlet. However, $\rho = 0.85$ and $\rho = 0.45$ seem to respectively be systematically above and below the literature values.

C. Compressibility

The compressibility, as given in eq. 15, has been studied for different sets of input parameters.

Figure 8 shows results for βP as a function of the density ρ , for different isotherms. Obtained results are compared to computational results from literature as well as to experimental measurements in argon. The behaviour of βP as a function of the density ρ is as expected for all isotherms. When the density of the system increases, the chance of particles running into each other increases. This leads to the system wanting to increase its volume. As the volume is fixed, however, the pressure increases. The same logic applies for increasing/decreasing the temperature. As the kinetic energy per particle increases or decreases the system will want to respectively expand or compress. As the volume is fixed this will instead either lead to an increase or a decrease in the pressure.

In general, our results are largely consistent with literature values for the isotherms $T = 2.74$ and $T = 1.35$, both regarding shape and values. For $T = 1.00$, while correctly estimating the shape of the literature curve, βP is, however, overestimated as a function of ρ . For all isotherms it seems that βP is estimated better for the relatively lower densities than for relatively higher densities. For these we find one or more overestimations for values of βP as a function of ρ for all isotherms.

We also studied the compressibility for constant density but varying temperature as presented in figure 9. First we see that, for all densities, the shape of the data points corresponds to the shape of the curves. However, the data points for $\rho = 0.45$ and $\rho = 0.85$ seem to respectively lie systematically below and

Table 2. Interaction part of the specific heat per particle for different values of ρ and T as well as the literature values determined by Lebowitz et al. [1].

ρ [-]	T [-]	C_i [-]	$C_{i_{theory}}$ [-]
0.85	2.89	0.771 ± 0.004	0.73
	2.20	0.792 ± 0.005	0.79
	1.21	0.964 ± 0.006	0.95
	1.13	1.055 ± 0.006	0.99
0.75	0.88	1.044 ± 0.009	1.11
	2.84	0.565 ± 0.004	0.56
	0.827	0.862 ± 0.006	0.88
0.45	4.62	0.181 ± 0.004	0.20
	2.93	0.214 ± 0.009	0.26
	1.71	0.301 ± 0.008	0.28
	1.51	0.384 ± 0.002	0.28

above the literature curves. No conclusions could be made on the origins of the overestimated values. For the underestimated values we think that this is due to values being close to or on a phase coexistence line.

D. Heat capacity

Firstly we check whether the heat capacity per particle approaches the expected value for high temperature, for argon this is around 2.8 based on Haenssler et al. [7]. The simulated value is 2.740 ± 0.004 for $T=1.2$ and $\rho = 0.85$. This strengthens the validity of the simulation.

Following the approach of Lebowitz et al. [1], the interaction part C_i of the specific heat is simulated for different values of ρ and T , the results are presented in table 2. To verify the validity of these results, we compare them to literature values ($C_{i_{theory}}$ by Lebowitz et al. [1]). The simulated values are close but not equal to the literature values. A first possible reason for this is that the $C_{i_{theory}}$ have an uncertainty of up to 20 percent. However, not every value has been assigned a specific uncertainty, making it hard to estimate the validity of the literature values. Furthermore, our experiment consisted of 500 particles while the literature reference used 864 particles. This is also a possible reason for the differences because more simulated particles means that the system is closer to the actual physical system.

Finally, different iterations of the same simulation also resulted in different values. We think that this is due to the rescaling of velocity as mentioned previously. Therefore, the energies will have different values resulting in different specific heats.

To get more accurate data in future simulations the first logical step is by making a bigger simulation i.e. more particles. Also employing more accurate models like 4th-order Yoshida integrators [13], instead of the velocity-Verlet algorithm, could prove useful.

E. Code performance

The simulation stored all calculated variables for every timestep. This approach was helpful for obtaining results, but prevented us from performing simulations of more than 500 particles. Memory errors arose the moment we simulated a system of 864 particles, due to the size of the initialised arrays. This error could easily be circumvented, f.e. by not storing all values for every timestep or by storing results in multiple arrays. Also, the simulation time increased exponentially with the amount of particles simulated, as can be seen in figure 10. Within the loop over all time, we also used a loop over all particles. By smart vectorisation this second loop should be easily eliminated, in order to optimize the efficiency of the simulation. While time was the limiting factor in integrating both of these modifications in our simulation, for further research we believe that these two improvements could bring about a significant boost in the performance of the simulation.

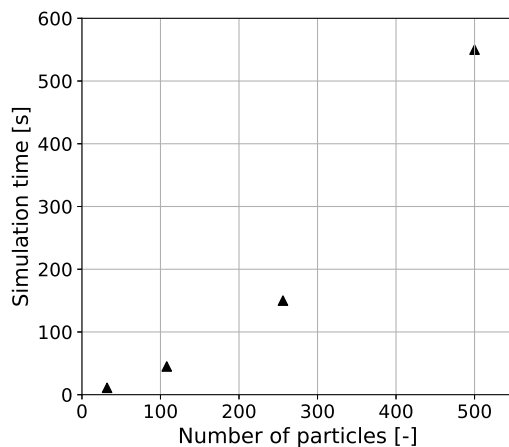


Fig. 10. Average simulation time as a function of the amount of particles simulated, for simulations of 5000 timesteps. As can be seen, the simulation time increases exponentially with the amount of particles. Simulation was performed with 8 GB of RAM and an Intel® Core™ i7-6700HQ CPU @2.6 GHz.

4. CONCLUSION

The results obtained from the simulation proved to be very accurate, showing expected behaviour for the total energy, the equilibrium temperature, the pair correlation function, the compressibility and the heat capacity of the system.

For enhanced future simulations, the system of argon particles should be enlarged by increasing the amount of simulated particles. To allow for these kind of simulations, the way data is stored should be modified. For enhanced performance the nested for-loop should be removed.

In future research also the diffusion of the particles in the system could be studied, as additional check to the validity of the simulation. The reader is welcomed to get in contact with the authors to get access to our code, to maybe extend upon the presented research.

REFERENCES

1. J. L. Lebowitz, J. K. Percus, and L. Verlet, "Ensemble dependence of fluctuations with application to machine computations," *Phys. Rev.* **153**, 250–254 (1967).
2. L. Verlet, "Computer "experiments" on classical fluids. i. thermodynamical properties of lennard-jones molecules," *Phys. Rev.* **159**, 98–103 (1967).
3. J. Jones, "On the determination of molecular fields. - . from the equation of state of a gas," *Proc. Royal Soc. Lond. Ser. A, Containing Pap. a Math. Phys. Character* **106**, 463–477 (1924).
4. J. M. Sanz-Serna, "Symplectic integrators for hamiltonian problems: an overview," *Acta Numer.* **1**, 243–286 (1992).
5. J. Thijssen, *Computational Physics* (Cambridge University Press, Kavli Institute of Nanoscience, Delft University of Technology, 2007). ISBN-13 978-0-521-83346-2.
6. J.-P. Hansen and I. R. McDonald, *Theory of Simple Liquids* (Academic Press, Oxford, 2013), fourth edition ed. ISBN: 978-0-12-387032-2.
7. F. Haenssler, K. Gamper, and B. Serin, "Constant-volume specific heat of solid argon," *J. Low Temp. Phys.* **3**, 23–28 (1970).
8. E. R. Hernández, "Molecular dynamics: from basic techniques to applications (a molecular dynamics primer)," in *AIP Conference Proceedings*, vol. 1077 (American Institute of Physics, 2008), pp. 95–123.
9. W. W. Wood and J. D. Jacobson, "Preliminary results from a recalculation of the monte carlo equation of state of hard spheres," *The J. Chem. Phys.* **27**, 1207–1208 (1957).
10. J. M. H. Levelt, "The reduced equation of state, internal energy and entropy of argon and xenon," *Physica*. **26**, 361 – 377 (1960).
11. W. Van Witzenburg, "The equation of state of liquid and solid argon," Ph.D. Thesis, Tor. Univ. (1963).
12. A. Itterbeek, O. Verbeke, and K. Staes, "Measurements on the equation of state of liquid argon and methane up to 300 kg cm² at low temperatures," *Physica*. **29**, 742–754 (1963).
13. H. Yoshida, "Construction of higher order symplectic integrators," *Phys. letters A* **150**, 262–268 (1990).